RSNA 2018
TOMORROW'S RADIOLOGY TODAY
104th Scientific Assembly and Annual Meeting
November 25–30 | McCormick Place, Chicago

There is fat!! What every radiologist needs to know about abdominal and pelvic fat-containing tumors and their mimics: a pictorial review

Viviane Brandão Amorim
Luiza Soares
Sheylla Medeiros
Rangel de Sousa
Eduardo Lemos
Rodrigo Paulino
Renata Perez
Rosana Rodrigues
Jaime Oliveira Neto
Daniella Parente

INCA INSTITUTO NACIONAL DE CÂNCER JOSÉ ALENCAR GOMES DA SILVA

GrupoFleury

Introduction

There are many abdominopelvic pathologic processes that can be accurately diagnosed depending on their imaging characteristics.

Frequently the image makes the diagnosis itself.

Demonstration of fat within a lesion at noninvasive imaging is an important clue to reduce the number of entities to be considered in the differential diagnosis.

Location of the fat-containing lesion is a critical parameter in formulating the correct diagnosis.

Learning Objectives

- Discuss and describe how to identify intralesional (macroscopic and microscopic) fat with CT and MR imaging techniques, in order to improve differential diagnosis.

- Review the radiological characteristics of the abdominopelvic tumors in which fat is the key to diagnosis.

- List the major differential diagnoses for the presence of fat in abdominopelvic tumors and their mimics by location.

What is Fat? How is fat defined?

- On Computed Tomography (CT), macroscopic fat have lower attenuation than water, defined by attenuation less than -20 Hounsfield Units (HU).
- On Magnetic Resonance (MR), macroscopic fat is hyperintense on T1-weighted and intermediately intense to hyperintense on T2- weighted fast spin-eco and gradient-echo images, but this aspect is not specific. Therefore, Fat Saturation (FS) techniques are very important for the most accurate identification, reducing the signal from lipid-containing voxels (macroscopic fat signal).

A- Demonstration of fat on CT image; B and C - Subcutaneous fat (green arrows) on T2W imaging (B) and T2FS (C)

What is Fat? How is fat defined?

Microscopic fat is best evaluated by Opposed-phase (OP) MR imaging, for lesions that contain both lipid and water on a cellular level, in which voxels with water and lipids lose the signal, characterizing the chemical shift artifact (black boundary or India ink artifact), seen in fat-water interfaces.

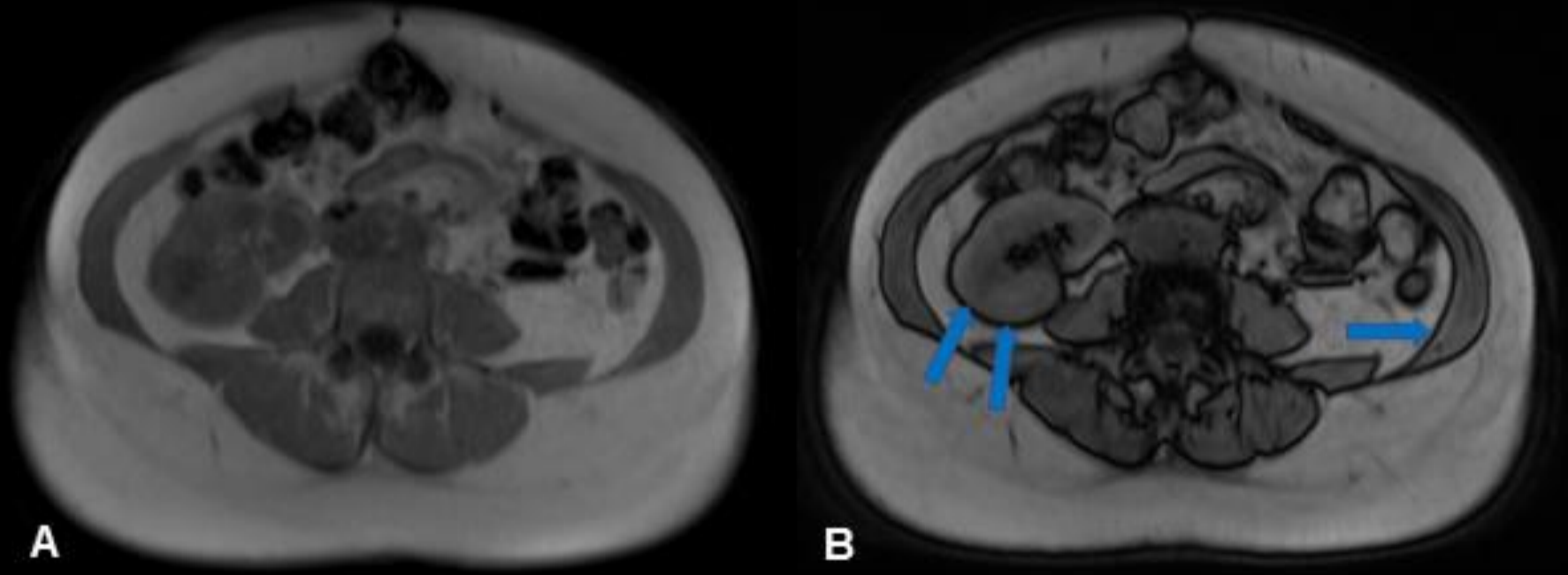

A and B - Demonstration of microscopic fat in "In and Out" of phase imaging: note the signal loss in the water-lipid interfaces, characterizing the chemical shift artifact (blue arrows).

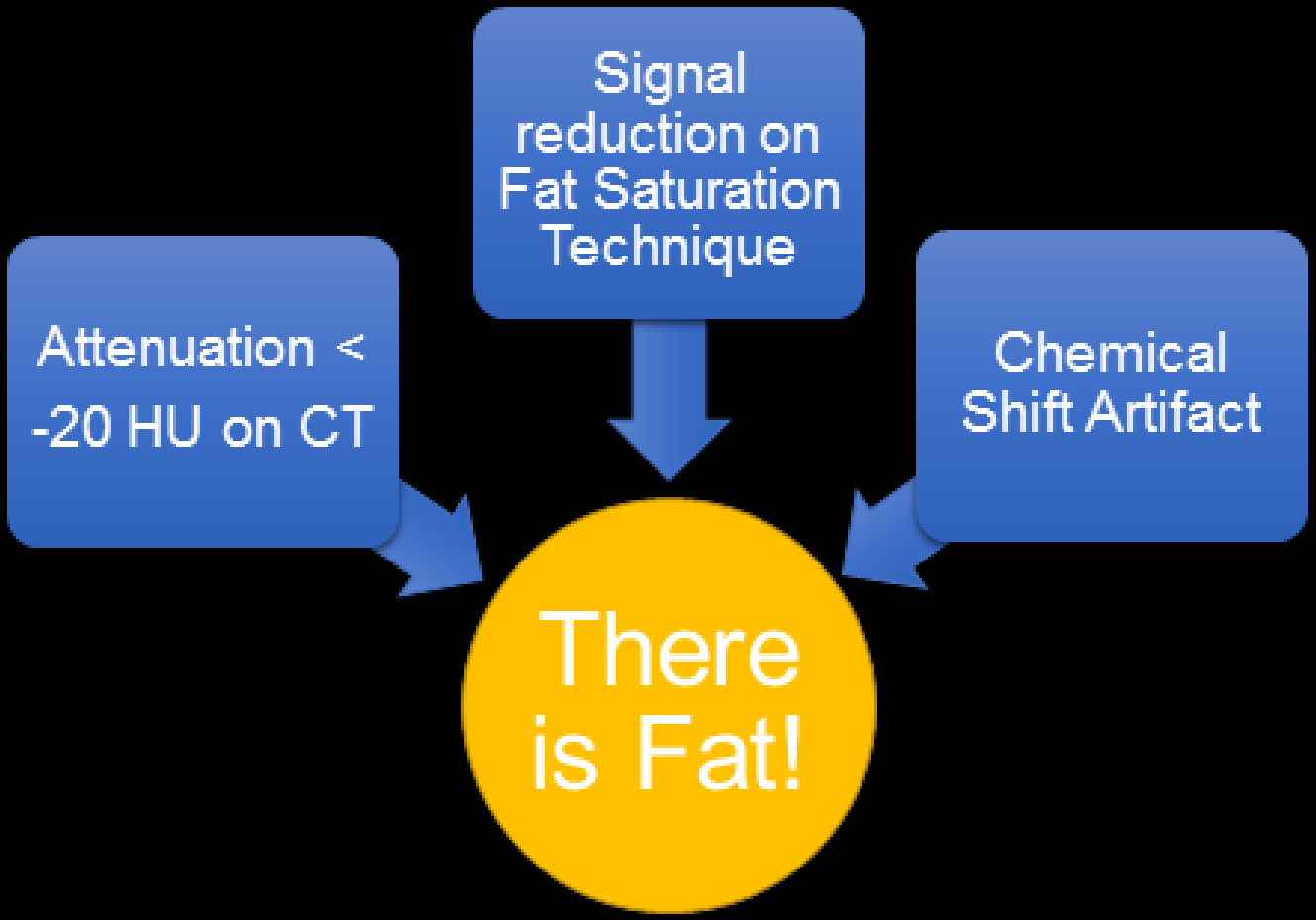

Now, we are going to discuss the main abdominopelvic lesions that contain macroscopic and/or microscopic fat, based on anatomical location.

Liver: Focal Fatty Deposition (Focal Steatosis)

Often recognized on typical location at periligamentous or periportal. Does not distort transverse blood vessels.

However, patchy focal fat deposition may be mistaken by an infiltrative neoplasm.

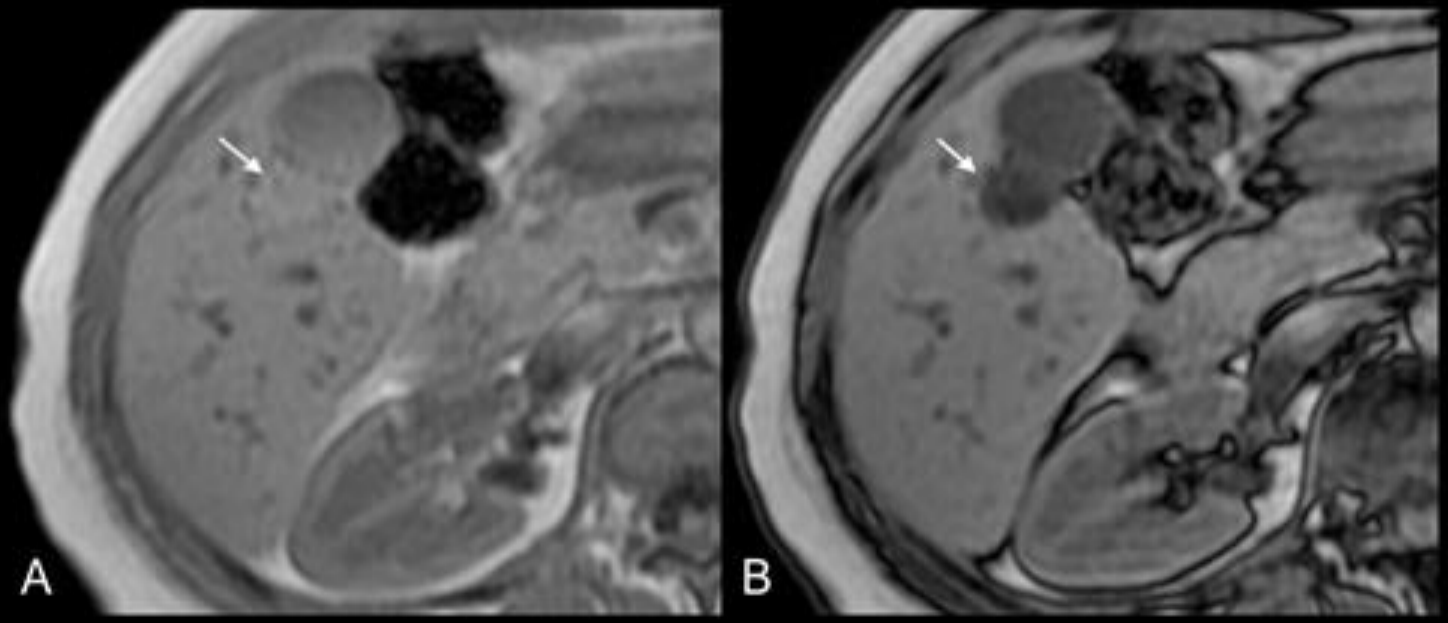

(A) in-phase and (B) opposed-phase GRE T1-weighted images show subcapsular nodular signal drop on opposed-phase image due to focal steatosis. There is poorly delineated margins and no mass effect.

Liver: Pseudolipoma of Glisson's Capsule

Encapsulated fat-containing lesion located within liver capsule.

Simple fat-containing nodule along surface of liver.

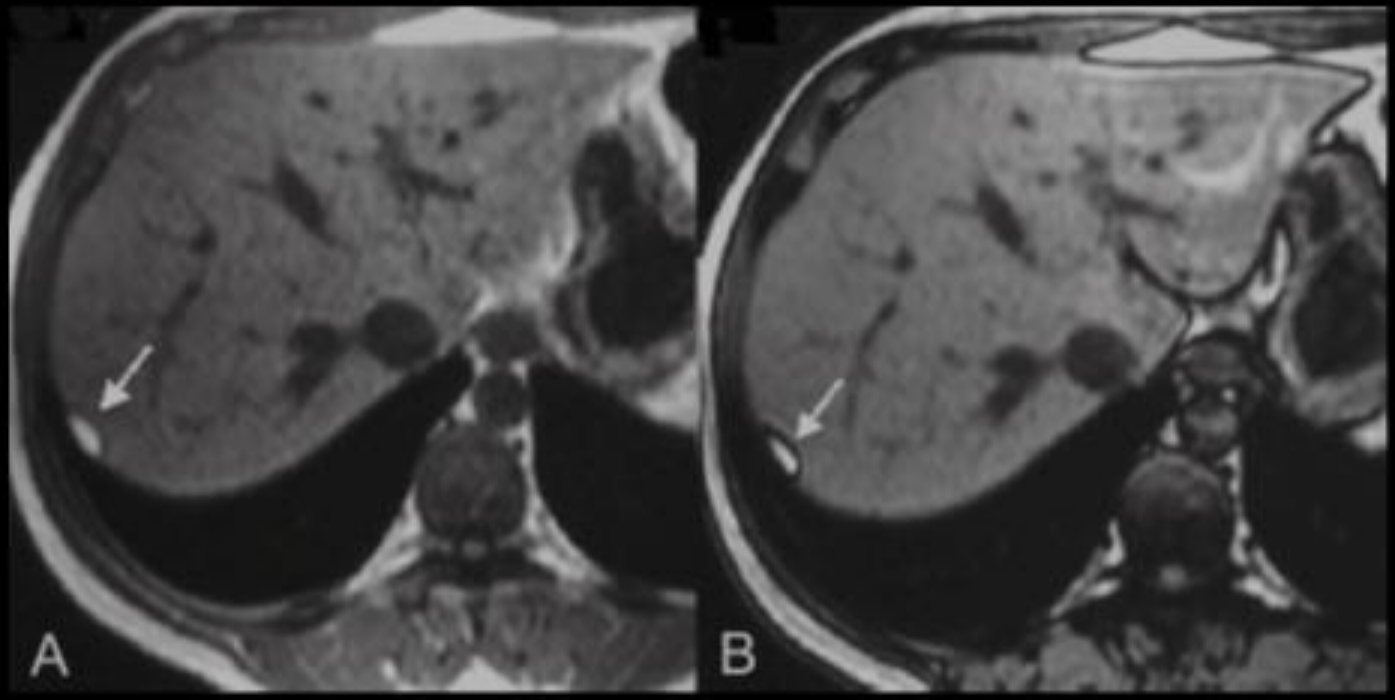

A: Axial in-phase T1-weighted GRE sequence shows a small subcapsular hyperintense lesion (arrow). B: Axial out-of-phase T1-weighted GRE image shows peripheral signal loss (arrow).

Liver: Steatotic regenerative nodules

Regenerative nodules are the most common nodules in cirrhotic livers.

Such nodules can contain fat and show high signal intensity on in-phase images and signal loss on out-of-phase images.

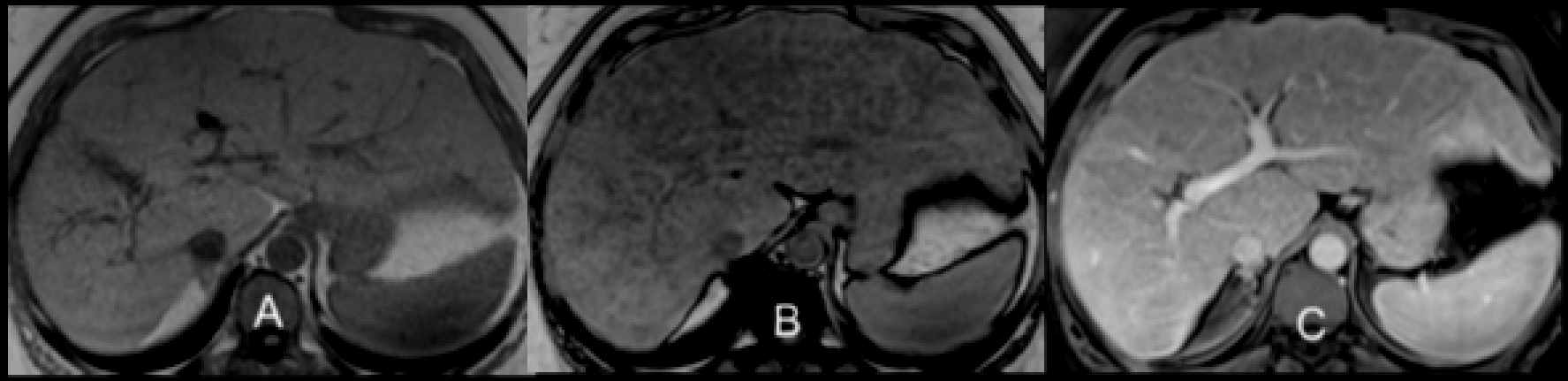

A: Axial T1-weighted image shows a cirrhotic liver, with volume increase of the caudate and left lobes, with nodular contour and heterogeneous signal intensity. B: Axial T1-weighted out-of-phase image demonstrates multiple diffuse small nodules with signal loss, characteristic of steatotic regenerative nodules. C: Axial T1-weighted image with fat saturation venous phase image shows nodule enhancement to the same degree as the adjacent liver.

Liver: Angiomyolipoma

Rare benign mesenchymal tumor composed of smooth muscle cells, blood vessels and mature adipose tissue.

Less associated to tuberous sclerosis (6%) compared to renal AML (20%).

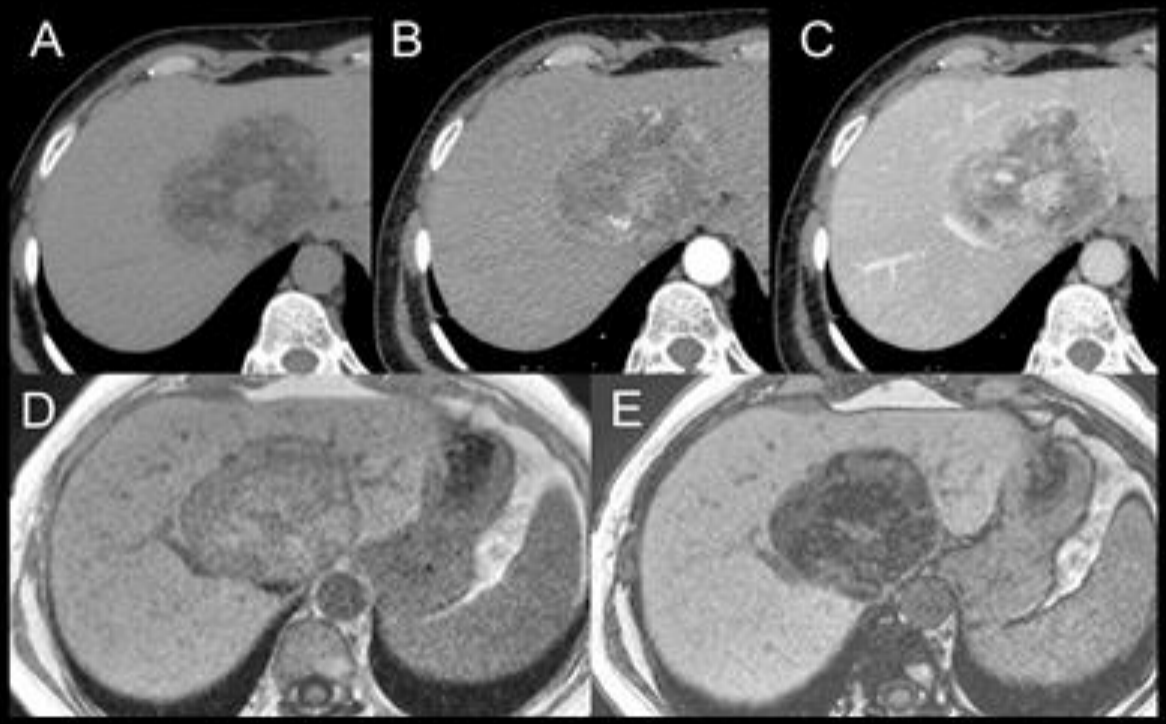

A: Non-enhanced CT (NECT) shows a mass with heterogeneous attenuation values due to the presence of fat and soft tissue densities. B (arterial phase) and C (portal phase): enhancement of vascular component in arterial phase (arrows). D: Axial in-phase T1-weighted GRE sequence shows a heterogeneously isointense lesion with focal areas of hyperintensity. E: Axial out-of-phase T1-weighted GRE sequence shows signal loss within the lesion.

Liver: Adenoma

Benign hepatic lesion with a propensity to hemorrhage and rare malignant change.

Most commonly occurs in young women taking oral contraceptives.

Only 7% of lesions demonstrate lipid deposition at CT.

However, 35-77% of out-of-phase images show signal loss in the fatty component.

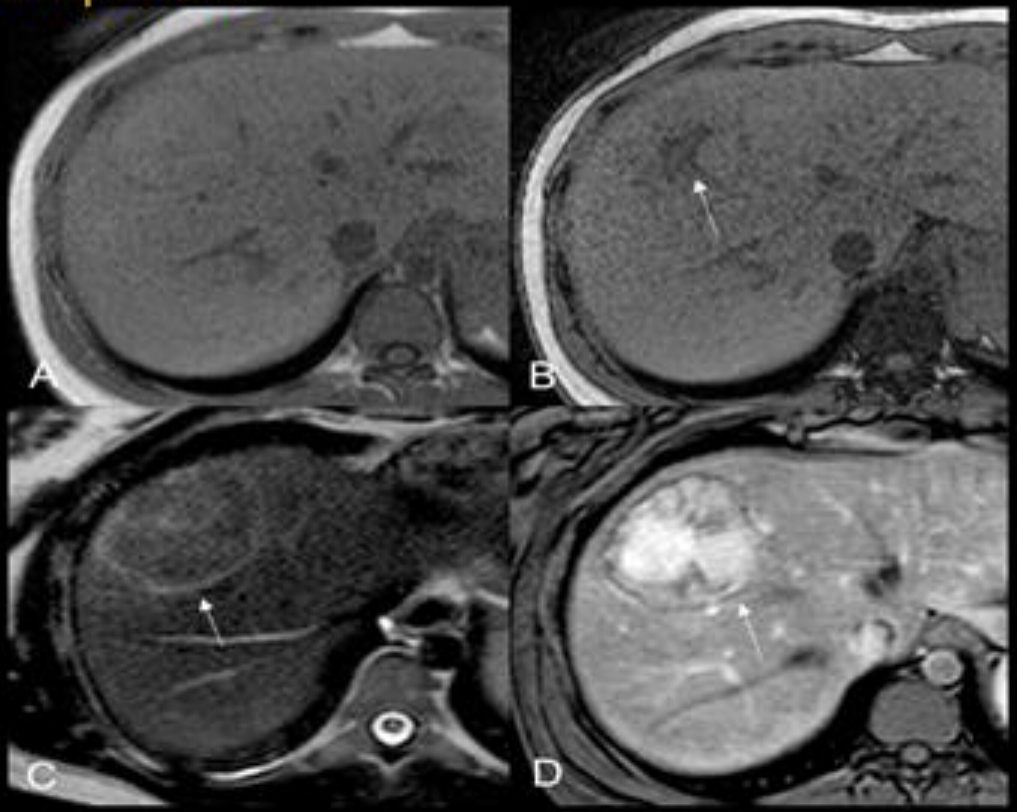

A: Axial in-phase T1-weighted GRE sequence shows a isointense lesion.
B: Axial out-of-phase T1-weighted GRE sequence shows focal areas of signal loss within the lesion (arrow).
C: T2-weighted MR image shows characteristic atoll sign of an inflammatory adenoma, which includes a T2-hyperintense signal band in the periphery of the lesion (like an atoll) with a center that is isointense to surrounding liver (like the surrounding sea).
D: On axial T1-weighted image with fat saturation arterial phase image the lesion demonstrates strong homogeneous enhancement.

Liver: Focal Nodular Hyperplasia

Second most common benign hepatic lesion, often discovered incidentally.

Occurs more in in young asymptomatic women.

The presence of fat is uncommon and usually associated with hepatic steatosis.

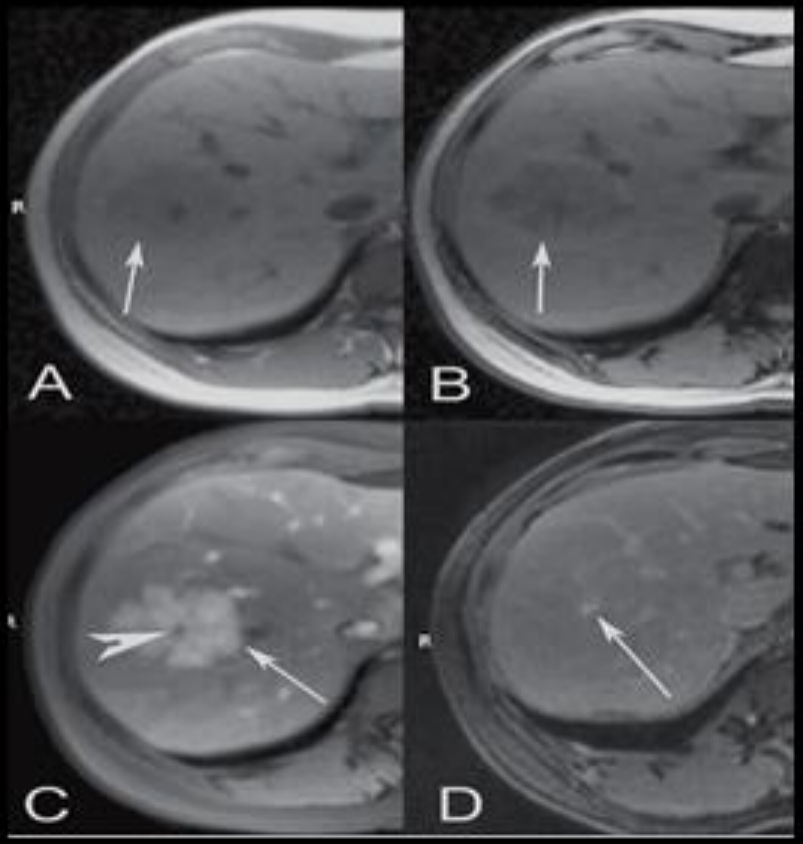

A: Axial in-phase T1-weighted GRE sequence shows a hypointense lesion (arrow).
B: Axial out-of-phase T1-weighted GRE sequence shows diffuse signal loss within the lesion (arrow).
C: Axial gadolinium-enhanced T1-weighted GRE arterial phase image shows intense homogeneous enhancement of the entire lesion (arrow), except for the central scar (arrowhead).
D: Axial gadolinium-enhanced T1- weighted GRE equilibrium phase image shows that the lesion has become isointense relative to the surrounding parenchyma, and that the central scar has enhanced (arrow).

Liver: Hepatocellular carcinoma

Commonest primary hepatic malignant neoplasm that commonly develops in a cirrhotic liver.

Fatty change can be seen in up to 35% of small HCCs and is associated with a decrease in the number of intratumoral arteries without any difference in intratumoral portal tracts.

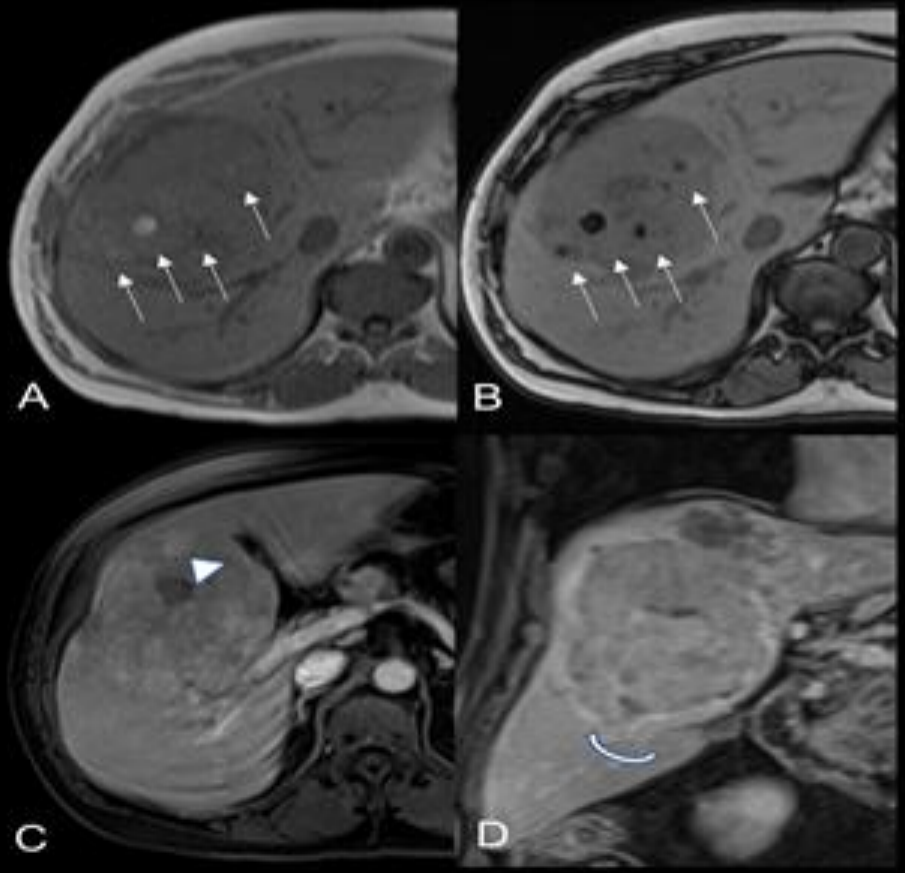

A: Axial in-phase T1-weighted GRE sequence shows a heterogeneously isointense lesion with focal areas of hyperintensity (arrows).
B: Axial out-of-phase T1-weighted GRE sequence shows focal areas of signal loss within the lesion (arrows).
C, D: On axial T1-weighted image with fat saturation arterial phase image (C), the lesion demonstrates strong heterogeneous enhancement with hypervascular foci (arrowhead) washout (D) and pseudocapsule enhancement (circle arrow).

Liver: Metastasis

In general, liver metastases do not contain fat.

Typically arise from liposarcomas and malignant germ cell tumors.

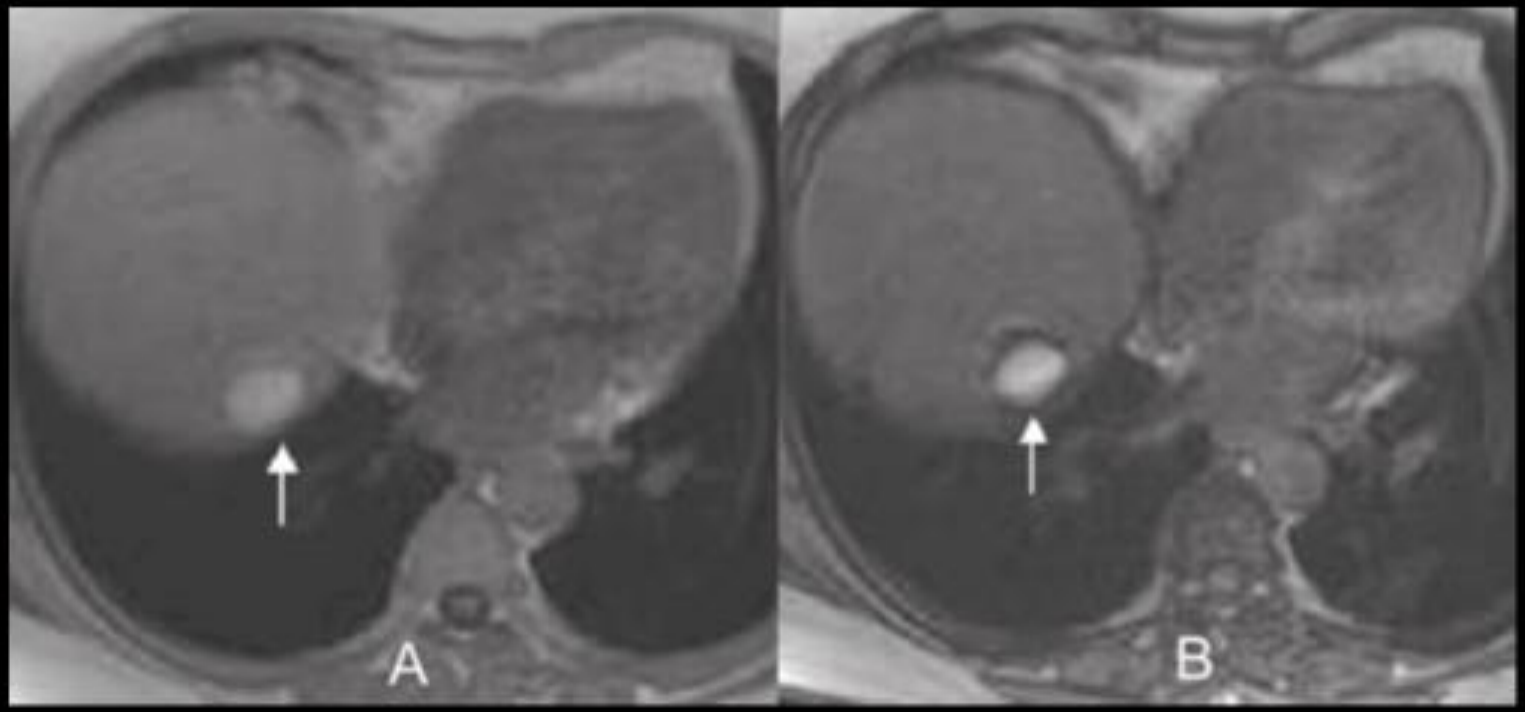

Teratocarcinoma metastasis from an ovarian source with peritoneal dissemination.
A: Axial in-phase T1-weighted GRE image shows a small hyperintense lesion on the hepatic dome (arrow).
B: Axial out-of-phase T1-weighted GRE sequence shows peripheral signal loss (arrow). Mild diffuse decrease in the signal intensity of the liver, due to steatosis is also observe.

Kidney: Angiomyolipoma

Most common benign renal neoplasm.

90% unilateral/ 10% bilateral.

Renal cortical mass with macroscopic fat, with variable proportion of muscle, fat and vessels.

5% are fat poor.

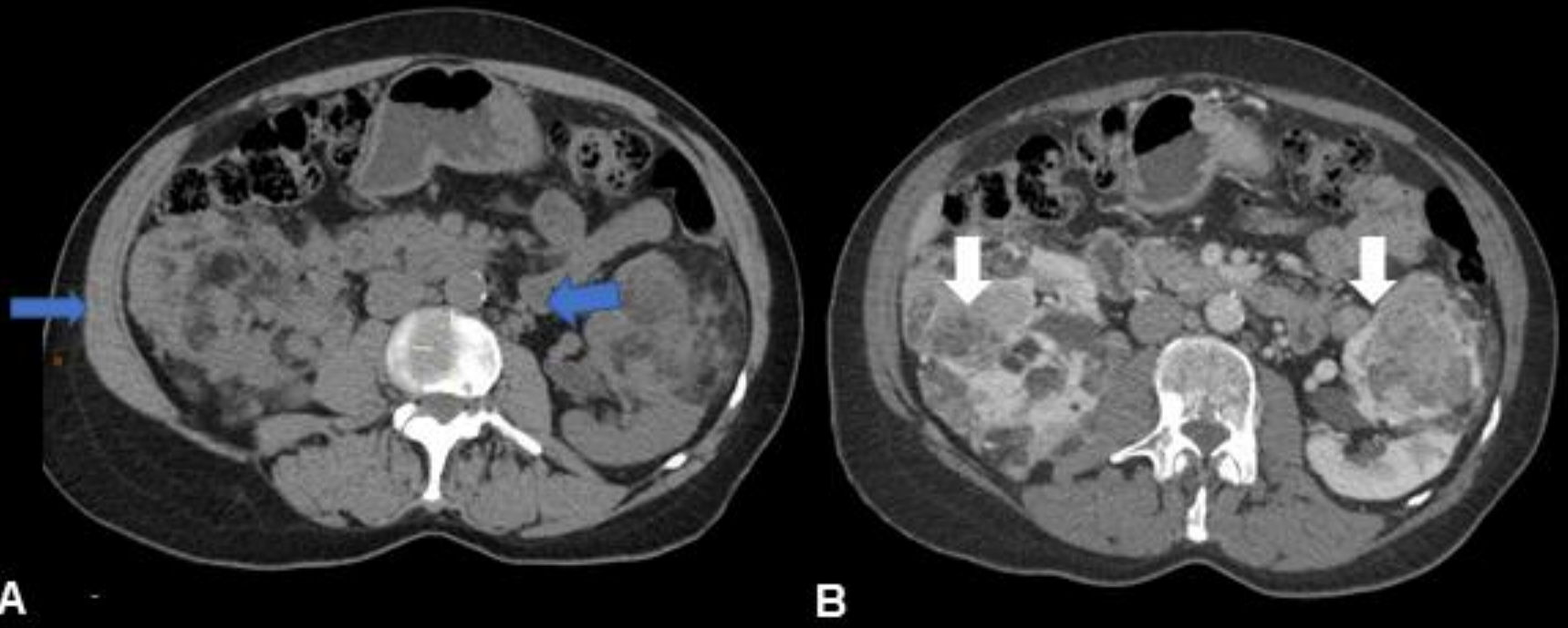

Axial NECT (A) and Contrast enhanced CT (CECT) (B) in a man with tuberous sclerosis, shows bilateral renal masses with macroscopic fat (blue arrows) and hypervascular areas (White arrows).

Kidney: Angiomyolipoma

Invasion of renal vein/IVC by AML is extremely rare.

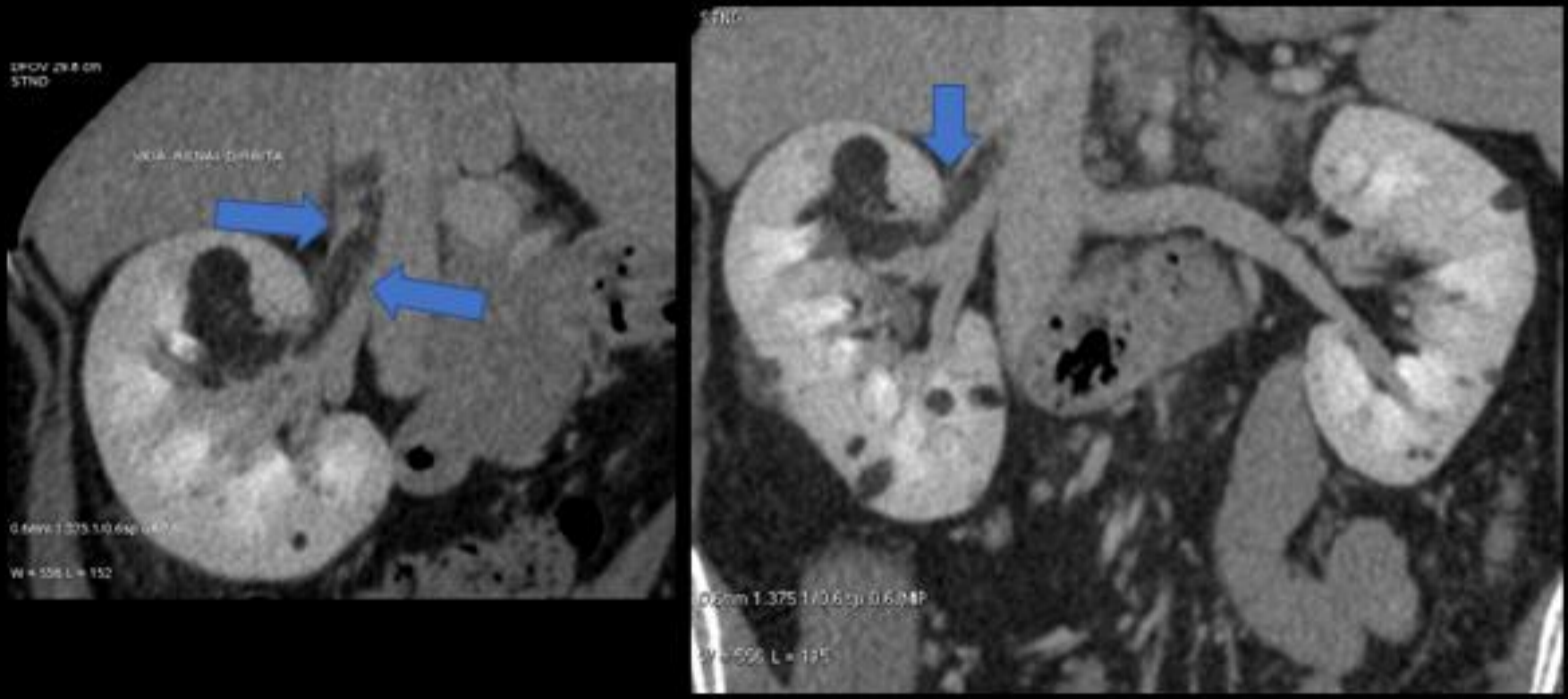

CECT on coronal planes, shows renal vein and IVC invasion by renal AML (Blue arrows), an extremely rare condition.

Kidney: Renal Cell Carcinoma (RCC)

Clear cell (70%), papillary (10-15%), granular cell (7%), chromophobe cell (5%).

Usually heterogenous hypervascular renal mass (clear cells).

May contain fat in a few cases.

The combination of fat and calcification suggests more RCC then angiomyolipoma.

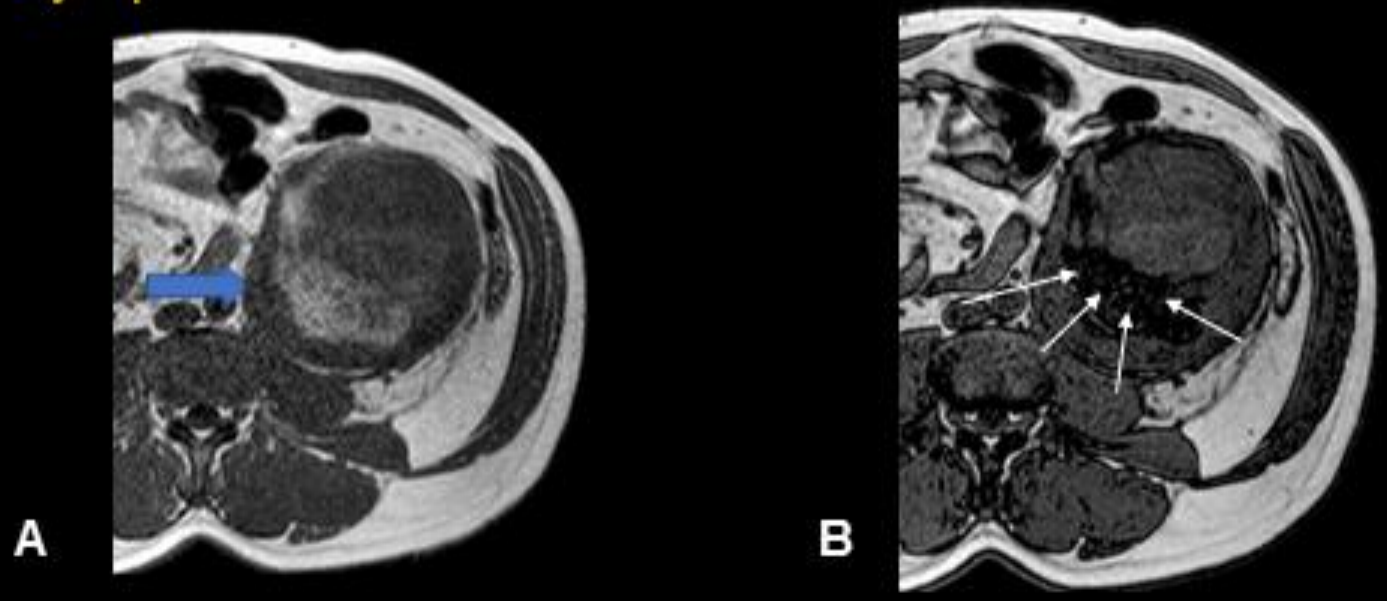

Fat-containing renal cell carcinoma. (A) Axial in-phase T1W - shows a heterogeneus left kidney mass, with area of high signal intensity (blue arrow), with respective low intensity (white arrows) on out-phase image (B), indicating microscopic fat.

Adrenal: Adenoma

Most common adrenal cortex tumor (>90% incidentalomas).

Round or oval, smooth, well defined adrenal mass.

Most lipid – rich (60-90%), with low attenuation (<10 HU) at NECT.

Loss of signal at out phase T1W imaging.

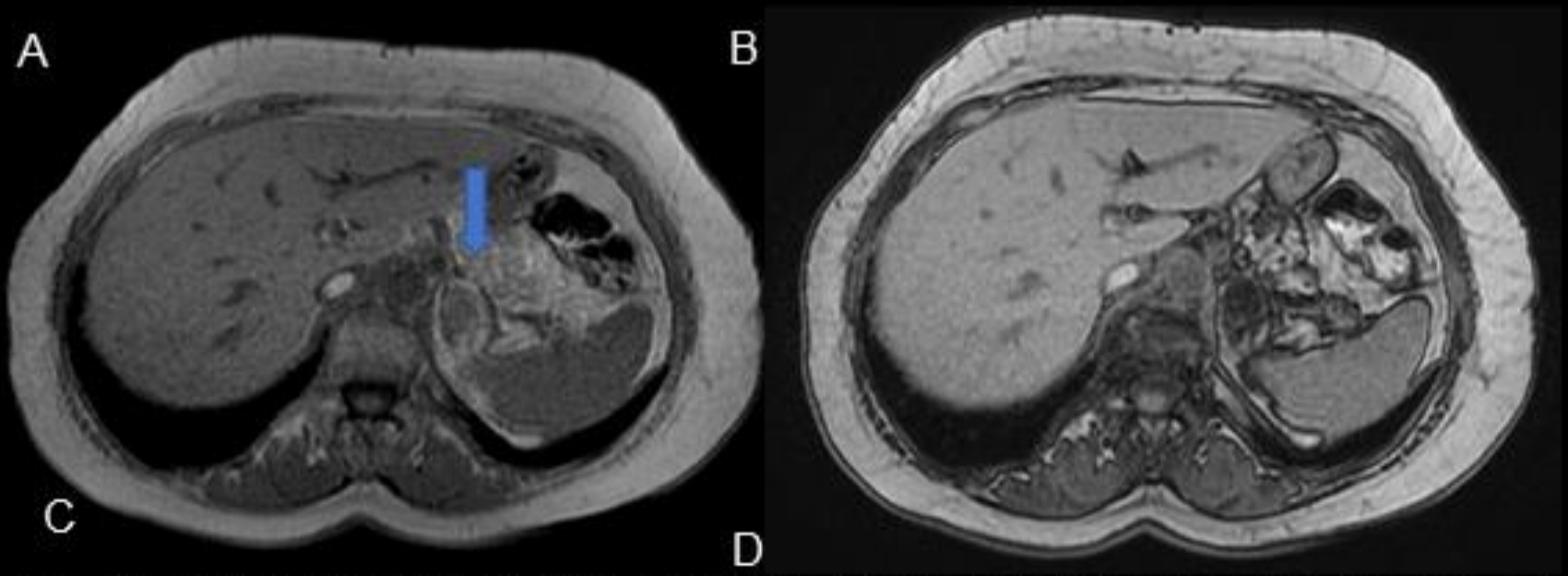

Axial (A) and coronal (B) NETC- shows a low attenuation (<10HU) right adrenal adenoma (B) T1W in phase MR- well-circumscribed, intermediate signal intensity left adrenal lesion (Blue arrow)(C) corresponding out phase image , shows uniform signal suppression of the left adrenal gland (white arrow). characteristic feature of lipid-rich adenoma.

Adrenal: Myelolipoma

Heterogeneous fat-containing adrenal mass.

Macroscopic fat within tumor is diagnostic.

The amount of fat is variable, of a foci to completely fat.

Interspersed "smoky" areas due presence of hematopoietic tissue.

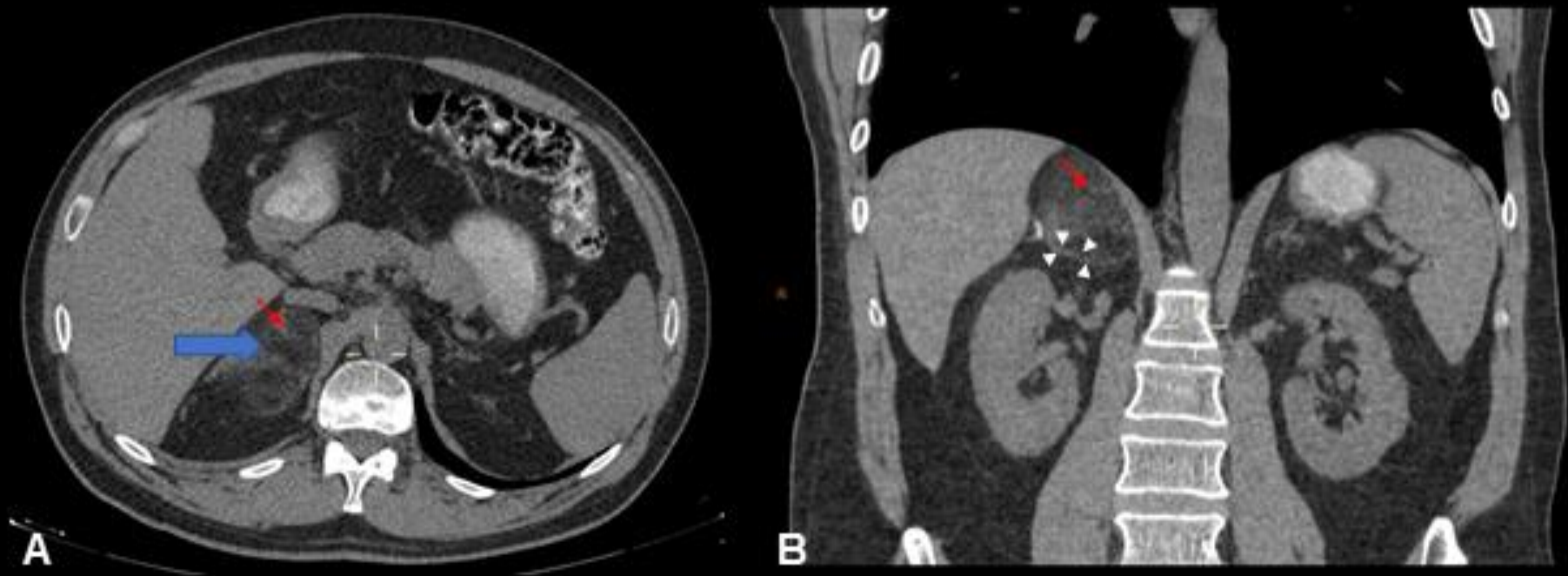

NECT in axial (A) and coronal (B) planes, shows a heterogenous, encapsulated (white arroweads), right suprarrenal mass (blue arrow) containg macroscopic fat and "smoky" areas (red arrows).

Pancreas: Pancreatic lipomatosis

Etiology of this entity is uncertain.

Most frequently in the elderly and obese populations.

Associated with diabetes mellitus, chronic pancreatitis, hepatic disease, dietary deficiency, viral infection, and steroid therapy.

Distribution of fatty infiltration is variable, with several reports citing the body and tail of the pancreas as the dominant areas of fatty replacement.

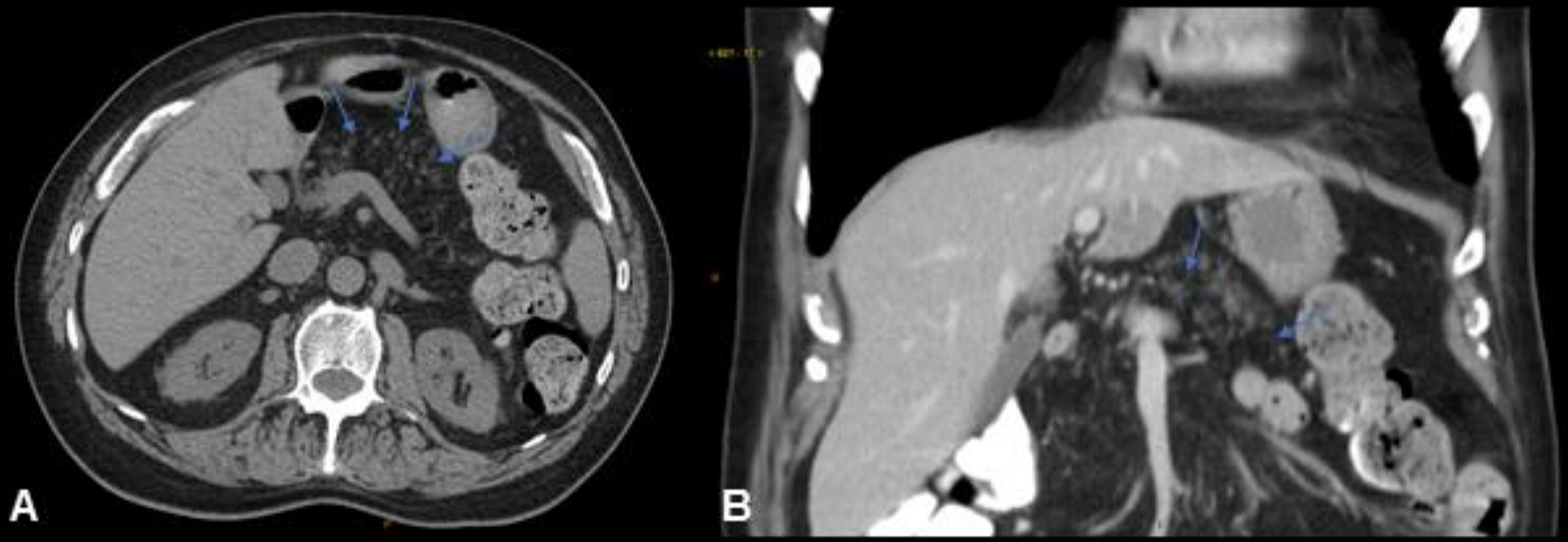

NECT on axial (A) and coronal (B) planes, shows extensive fatty infiltration of the pancreas (blue arrows)

Pancreas: Lipoma

Benign mesenchymal tumor that resembles normal fat.

The imaging shows as well-defined, homogeneous lesions without infiltration of peripancreattic fat, widening of the pancreatic duct.

May arise in any region of body that contains fat.

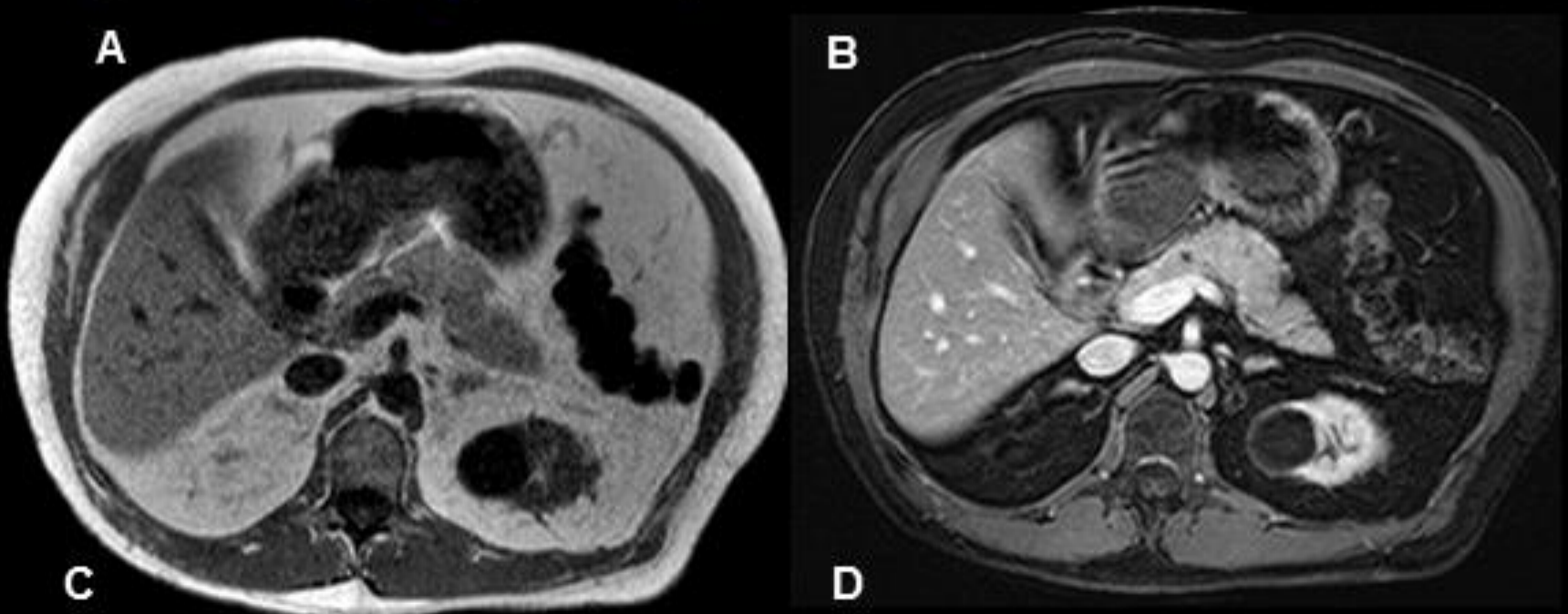

Axial NECT (A) and CECT(B)- Foci of fat in corporal and caudal portions of pancreas (blue arrows). In T1W (C) and T1WFS C+ (D) MR images confirm the presence of macroscopic fat.

Ovary: Teratoma

Most common germ cells tumor.

Mature cystic teratomas - Dermoid cysts.

Contains variable amounts of fat, soft tissue, fluid, calcification or bone.

Adipose tissue is seen in 67-75% of the cases.

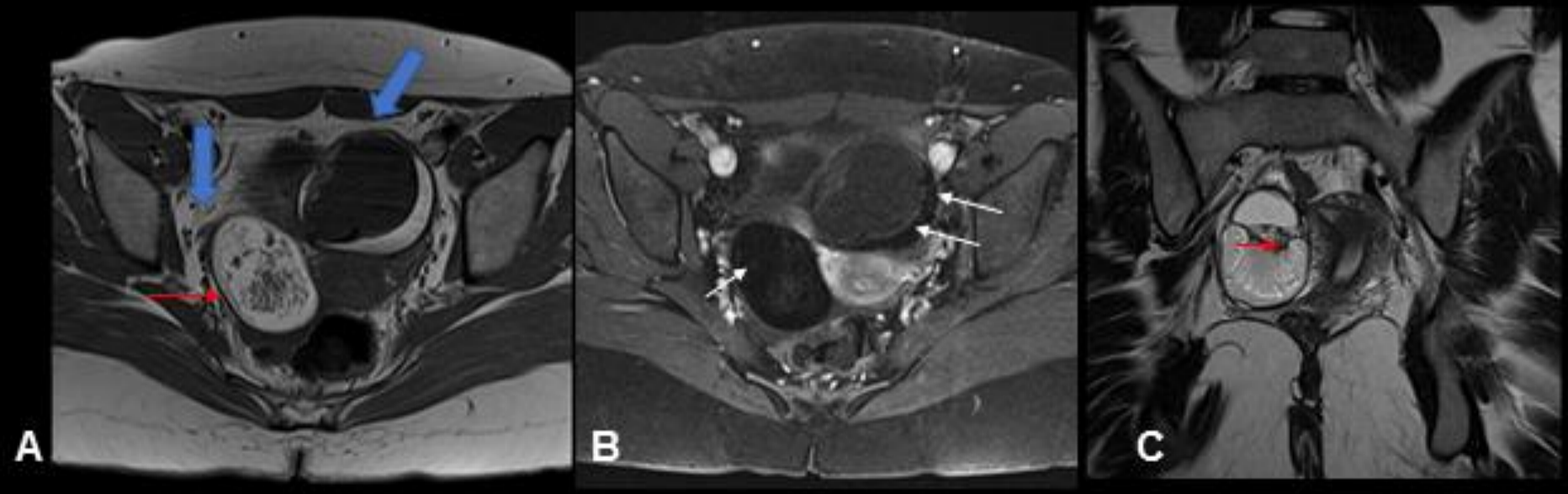

Axial T1W (A) e T1WFS with contrast (B) and T1W coronal plane (C) shows heterogenous ovarian masses (blue arrows) with macroscopic fat (marked signal loss relative to the signal intensity on the in-phase image- White arrows) and thin soft tissue components (red arrows) .

Uterus: Lipoleiomyoma

Rare benigne uterine tumor composed entirely, or in part, of adipose tissue, with intermixed smooth muscle.

Defined by fat-containing, well-marginated mass of uterus.

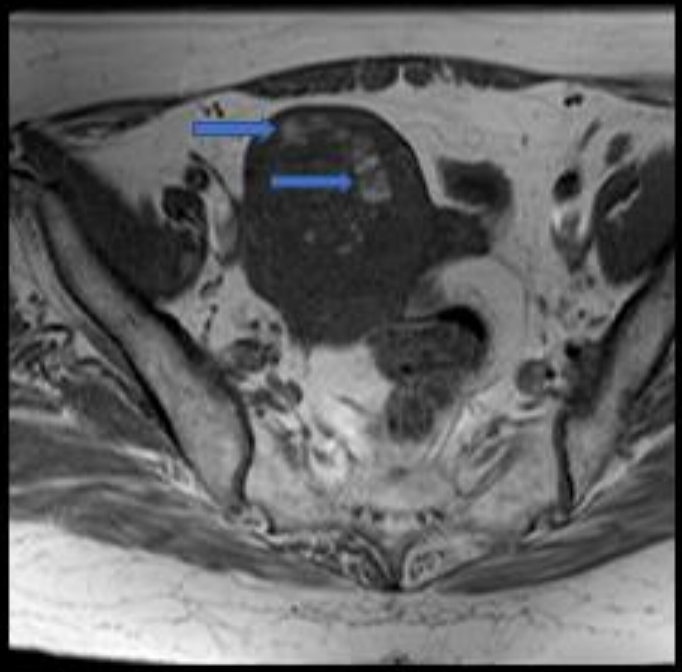

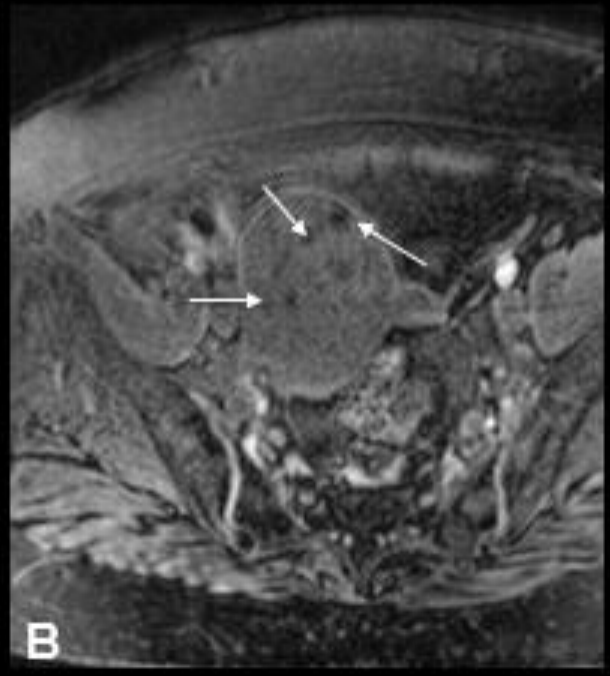

A- Axial T1W (A) and T1WFS shows a round, well defined, heterogeneus mass, with hyperintense areas (blue arrows) that lose the signal on FS (White arrows), characterizing macroscopic fat.

Bowel: Lipoma

The colon is the most commonly affected bowel segment, (65%–75)% of gastrointestinal lipomas.

Homogeneous fatty attenuation at CT.

A B

CECT images with oral contrast, on axial (A) and coronal planes (B) shows well defined, intraluminal mass in ascending colon(blue arrows), with homogeneous fat density, characterizing colonic lipoma.

Bowel: Intussusception

Invagination of proximal segment of bowel (intussusceptum) into lumen of distal segment (intussuscipiens).

Often contains some mesenteric fat attached to the involved segments of bowel.

Location: Ileoileal > ileocolic > colocolic.

CT shows alternating layers of mesenteric fat and soft tissue density bowel walls.

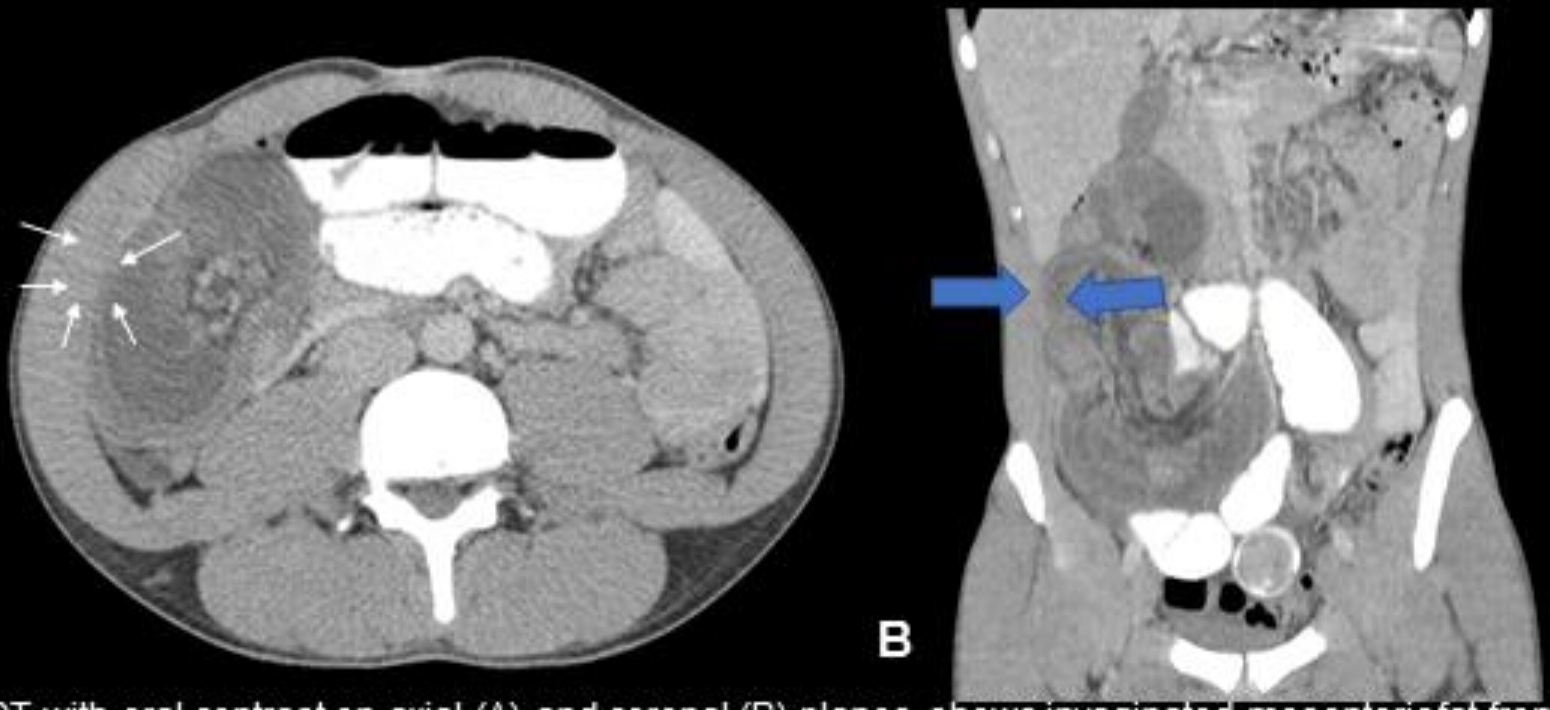

CECT with oral contrast on axial (A) and coronal (B) planes, shows invaginated mesenteric fat from an ileocolonic intussusception (Blue arrows). Note the mesenteric vessels surrounded by mesenteric fat (White arrows).

Retroperitoneum: Liposarcoma

Malignant tumor of mesenchymal origin.
May arise in any fat-containing region of the body.
Most common primary retroperitoneal malignant tumor.
Myxoid liposarcoma is the most common subtype, accounting for 50% of all liposarcomas.
Variable CT appearance, from a solid-tissue pattern with minimal fat to a mixed pattern of predominantly fat attenuation with areas of higher attenuation tissue.

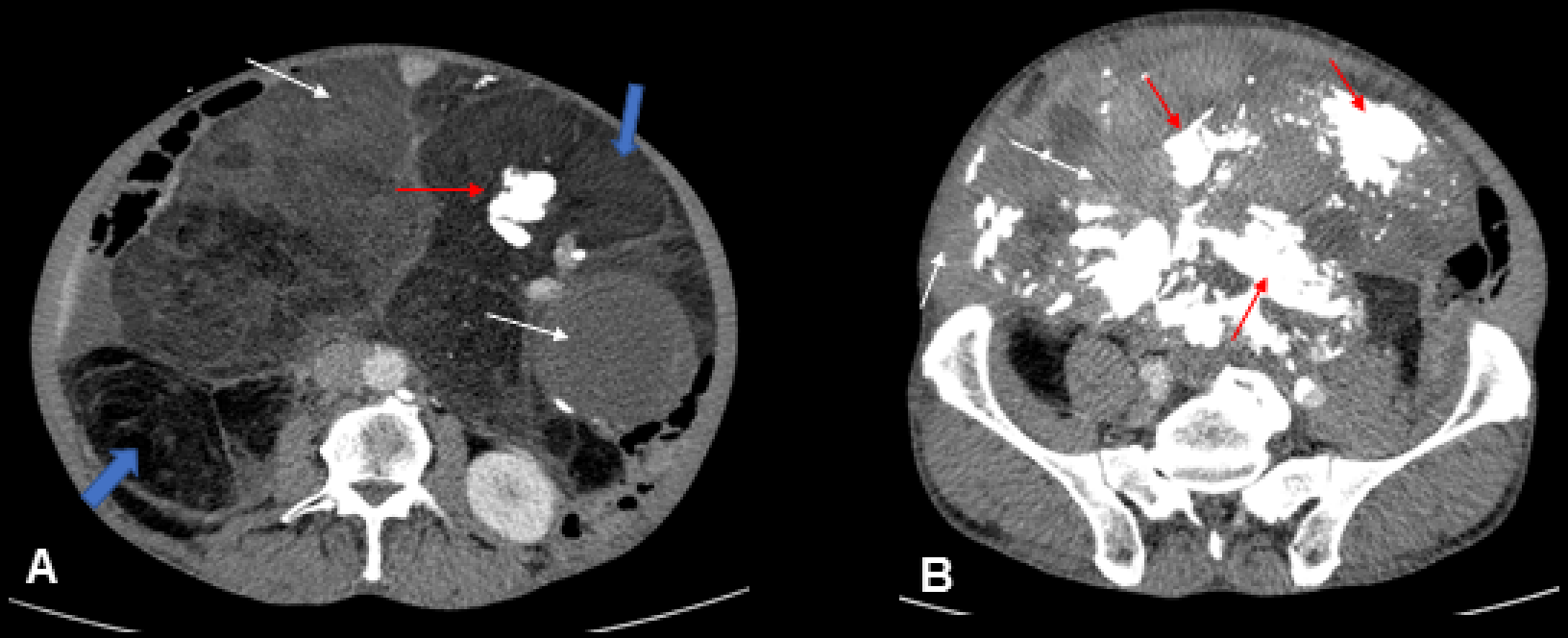

Axial CECT of uper abdomen (A) and pelvis (B) from the same patient, shows a large retroperitoneal mass, with macroscopic fat (blue arrows), calcified areas (red arrows) and soft tissue solid areas representing myxoid degeneration (White arrows).

Peritoneal Cavity: Epiploic appendagitis

Acute inflammation or infarction of epiploic appendages, resulting from torsion or occlusion of central vessel of appendage.

Pericolonic oval fat-containing mass, with hyperattenuating ring, usually anterior or anterolateral to the adjacent colon.

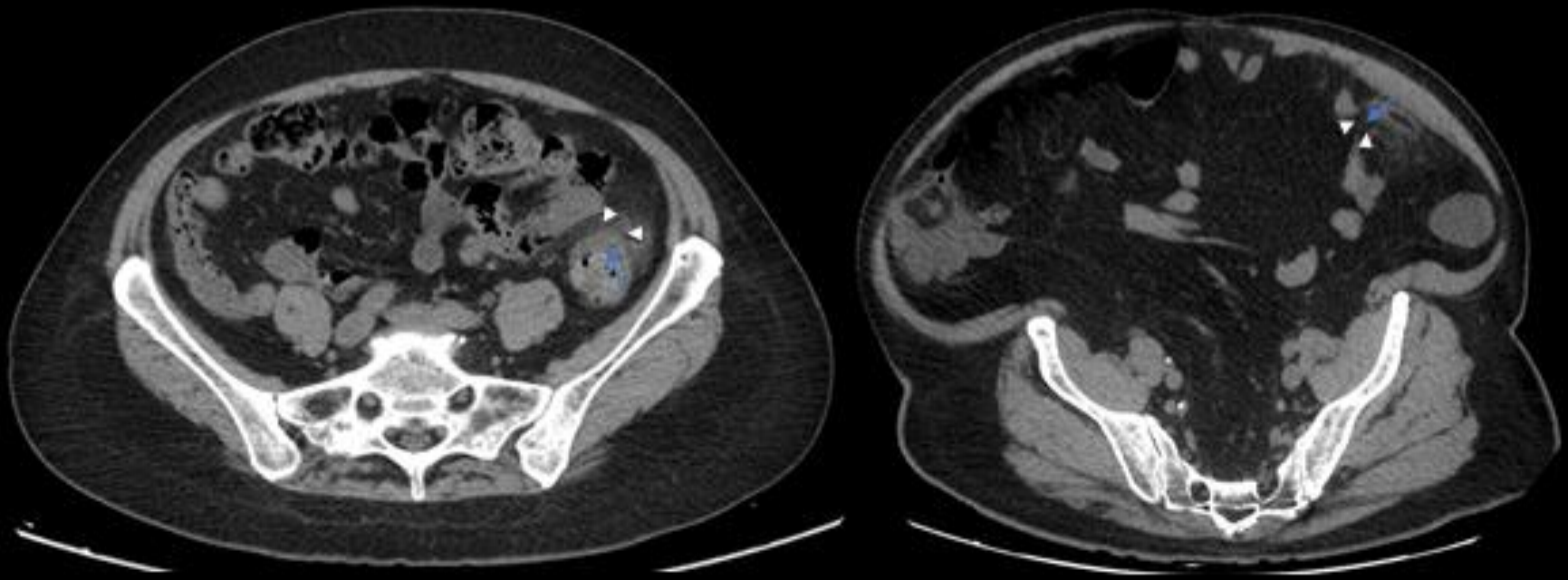

Axial CECT of two patients with left low quadrant pain, shows a small oval foci of fat (blue arrows) surrounded by a hyperdense rim (white arrowheads) and descending colon mesenteric stranding, caused by torsion and infarction of the epiploic appendages.

Peritoneal Cavity: Omental infarct

Most common on right lateral free edge of the omentum.

Primary or secondary causes.

Primary is often resulting from vascular compromise.

Secondary omental infarction may occur after a traumatic injury as a result of surgical trauma or inflammation of the omentum.

CECT on axial (A) and coronal (B) planes shows an ovoid focus of fat stranding (blue arrows) adjacent to hepatic flexure of the colon. Note the hyperattenuating streaky densities due to fibrous bands or thrombosed vessels (white arrows)

Peritoneal Cavity: Encapsulated Fat Necrosis

May occur anywhere in the body.

Result from a traumatic or ischemic insult that causes fat degeneration.

The necrotic fatty tissue organizes within a thin or thick fibrous capsule.

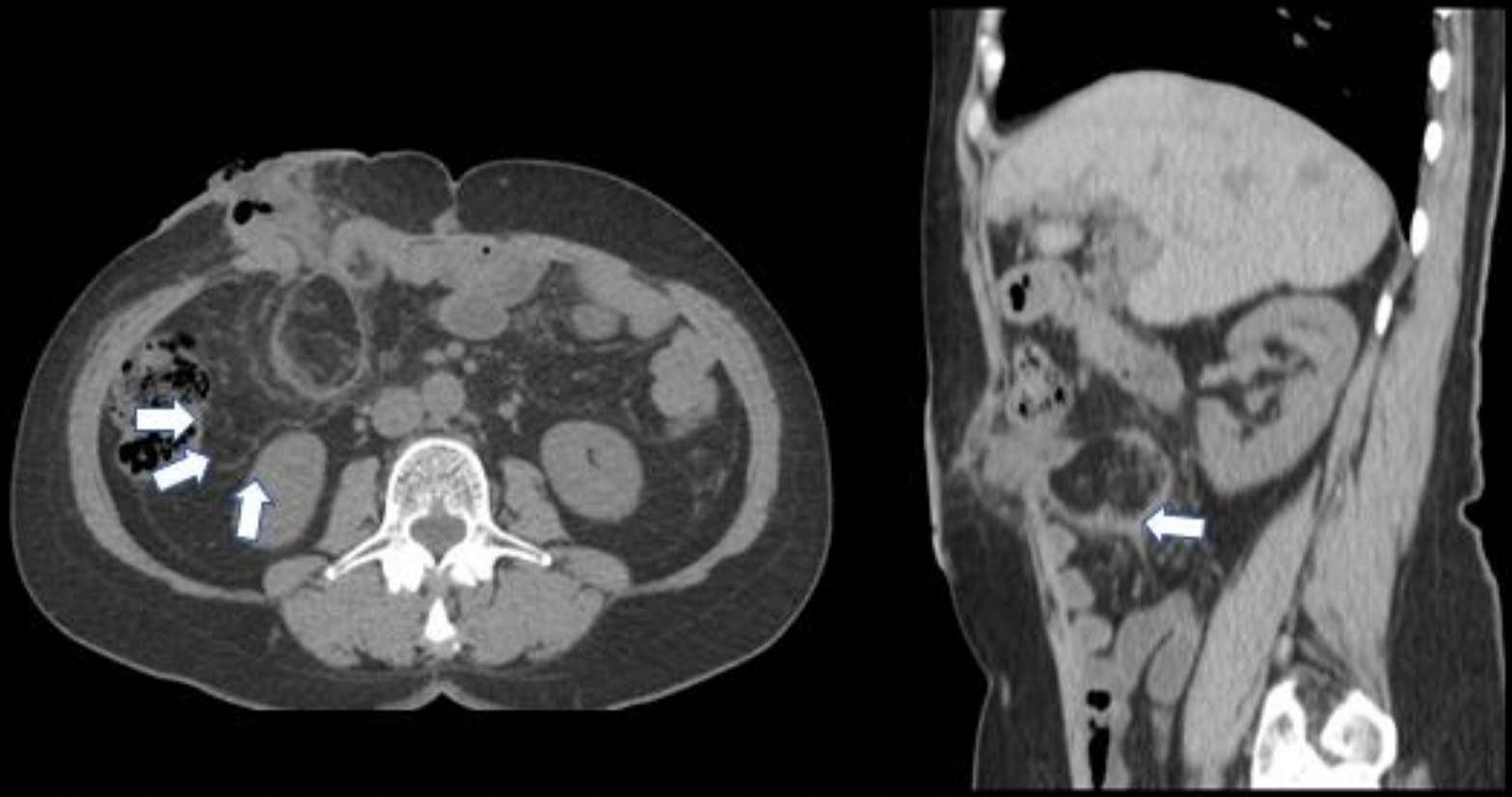

Axial (A) and Sagital (B) NECT shows aound, encapsulated lesion (blue arrows), in the right side of the abdomen, with a central area of fat attenuation. Etiology of this case is related to colostomy procedure.

Peritoneal Cavity: Sclerosing mesenteritis

Rare, benign and chronic fibrosing inflammatory disease.

Affects the adipose tissue of the mesentery of the small intestine and colon;

The specific etiology of the disease is unknown.

Often contains multiple prominent subcentimeter lymph nodes with halo of surrounding spared fat.

Envelops vasculature without narrowing or attenuation.

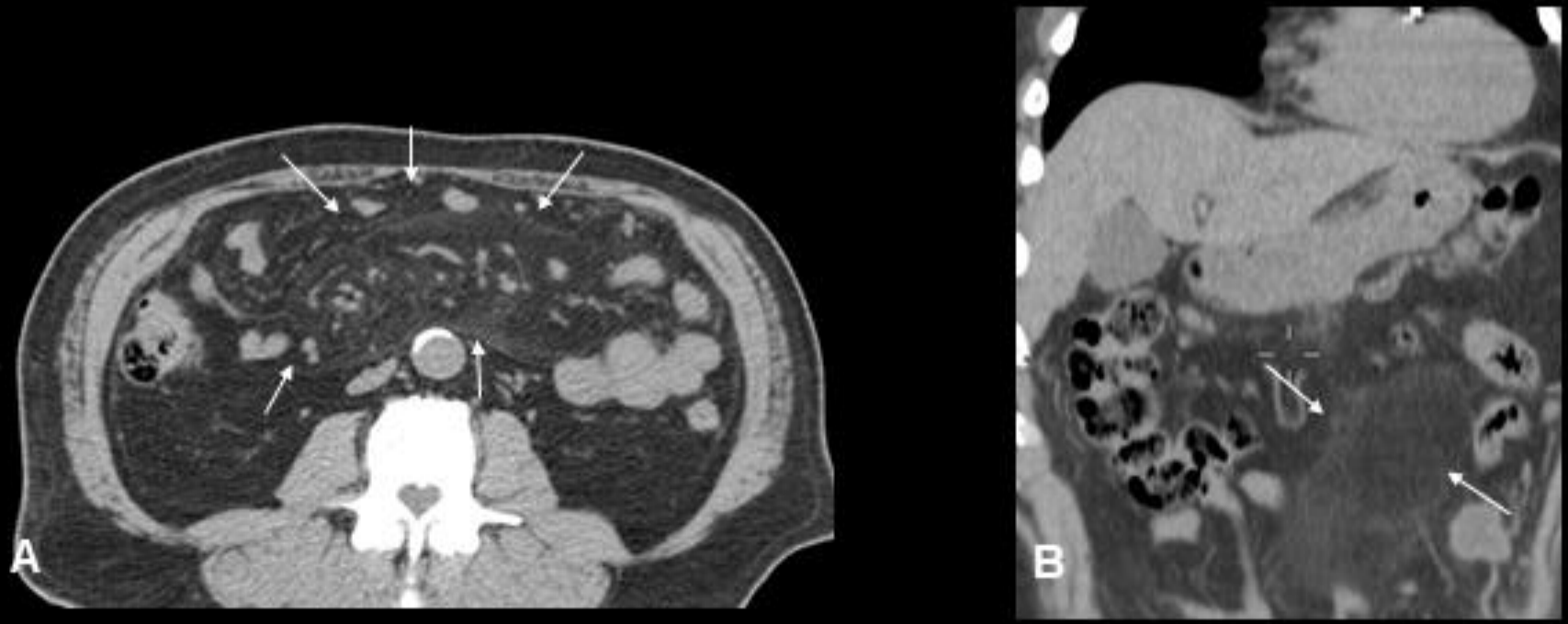

Axial (A) and coronal (B) NECT, shows infiltration of jejunal mesentery demarcated by a pseudocapsule (White arrows).

Abdominal Wall: Hibernoma

Rare, benign tumor of brown adipose tissue.

Well-defined mass in middle-aged patient.

Most common in thigh (30%).

Signal intensity similar to, but not exactly matching, subcutaneous fat.

Diagnosis is often not possible based on imaging alone.

Abdominal Wall: Metastasis

Most common primary are melanoma, lung, breast and renal cell due hematogenous spread.

Some aspects similar to primary tumor, including presence of fat.

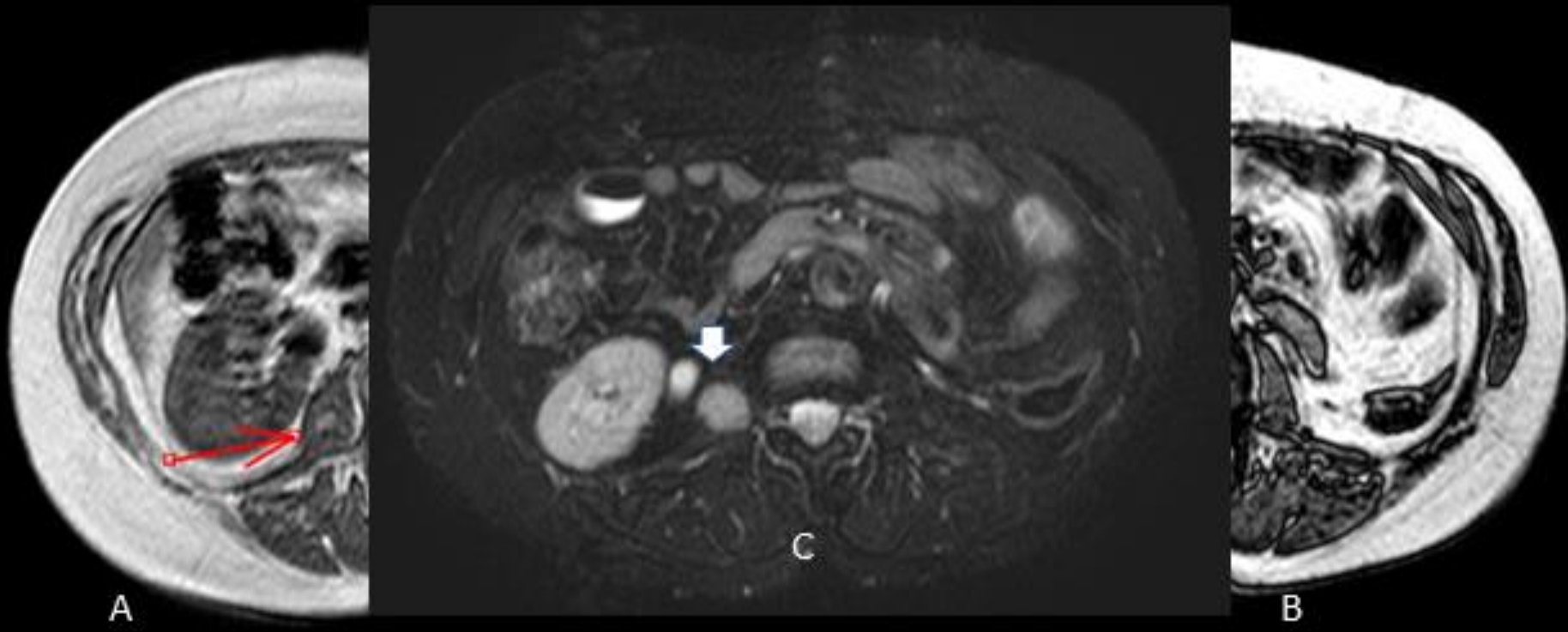

Psoas Muscle Metastasis (RCC). In (A) and out phase (B) axial T1W images, shows round mass in right psoas muscle, with central hyperintense foci (red arrow) with corresponding low signal in out phase image (green arrow), indicating microscopic fat. Note the hipervascular pattern on T1WFS C+ (C) (White arrow).

Take Home Message

- The presence of fat in an abdominal or pelvic lesion tends to limit the differential diagnosis.
- Although CT allows easy identification of macroscopic fat, it is not as reliable for lesions with microscopic fat.
- MR imaging techniques like fat saturation and chemical shift are good tools for evaluation of this lesions.
- The location of the fatty lesion is crucial to the correct interpretation of the imaging findings.

References

Pereira JM, Sirlin CB, Pinto PS, Casola G. CT and MR Imaging of Extrahepatic Fatty Masses of the Abdomen and Pelvis: Techniques, Diagnosis, Differential Diagnosis, and Pitfalls. RadioGraphics 2005 Jan-Feb; 25(1): 69-85.

Fultz PJ, Hampton WR, Skucas J, Sickel JZ. Differential Diagnosis of Fat-containing Lesions with Abdominal and Pelvic CT . RadioGraphics 1993 Nov; 13(6):1266-80.

Ariza MVT et al. In fat we trust: abdominal and pelvic fat containing lesions. ECR 2013, C-1278. DOI: 10.1594/ecr2013/C-1278.

Kamaya A, Federle MP, Desser TS. Imaging Manifestations of Abdominal Fat Necrosis and Its Mimics. RadioGraphics 2011 Nov-Dec; 31(7): 2021-34.

Shin NY et al. The Differential Imaging Features of Fat-Containing Tumors in the Peritoneal Cavity and Retroperitoneum: the Radiologic-Pathologic Correlation. Korean J Radiol 2010 May-Jun; 11(3): 333-45.

Cogley JR et al: MR imaging of benign focal liver lesions. Radiol Clin North Am. 52(4):657-82, 2014

Prasad SR et al. Fat-containing Lesions of the Liver: Radiologic-Pathologic Correlation. RadioGraphics 2005 Mar-Apr; 25(2): 321-31.

Costa, A. F., Thipphavong, S., Arnason, T., Stueck, A. E., & Clarke, S. E. (2018). Fat-Containing Liver Lesions on Imaging: Detection and Differential Diagnosis. American Journal of Roentgenology, 210(1), 68–77. doi:10.2214/ajr.17.18136

Kang SK et al: Solid renal masses: what the numbers tell us. AJR Am J Roentgenol. 202(6):1196-206, 2014

Lattin GE Jr et al: From the radiologic pathology archives: Adrenal tumors and tumor-like conditions in the adult: radiologic-pathologic correlation. Radiographics. 34(3):805-29, 2014

Shaaban AM et al: Ovarian malignant germ cell tumors: cellular classification and clinical and imaging features. Radiographics. 34(3):777-801, 2014

Williamson JM et al: Small bowel tumors: pathology and management. J Med Assoc Thai. 97(1):126-37, 2014

Hekimoglu K: Giant retroperitoneal liposarcomas: diagnostic approach with multidetector computed tomography and magnetic resonance imaging. JBR-BTR. 96(6):375-7, 2013

Park TU et al: Omental infarction: case series and review of the literature. J Emerg Med. 42(2):149-54, 2012

Potts J et al: Small bowel intussusception in adults. Ann R Coll Surg Engl. 96(1):11-4, 2014

Liu W et al: Fibermoma: comparing imaging appearance with more commonly encountered benign or low-grade lipomatous neoplasms. Skeletal Radiol. 42(8):1073-8, 2013